Toughening of Poly(lactic acid) with the Renewable Bioplastic Poly(trimethylene malonate)

Ersan Eyiler,[1] I-Wei Chu,[2] Keisha B. Walters[2]

[1]Department of Chemical Engineering, Cukurova University, Ceyhan, Adana 01950, Turkey
[2]Dave C. Swalm School of Chemical Engineering, Mississippi State University, Mississippi State, Mississippi 39762
Correspondence to: K. B. Walters (E-mail: kwalters@che.msstate.edu)

ABSTRACT: The aim of this work was to enhance poly(lactic acid)'s (PLA) flexibility and ductility by blending it with another bioplastic. Poly(trimethylene malonate) (PTM), developed as part of this study, was synthesized from 1,3-propane diol and malonic acid via melt polycondensation. Blend films of PLA and PTM were prepared by solvent casting from chloroform. Differential scanning calorimetry and thermogravimetric analysis were used to show shifted phase transitions and a single glass-transition temperature, indicating miscibility of PTM in the blend films. Morphology and mechanical characterizations of the PLA/PTM blend films were performed by atomic force microscopy using a quantitative nanomechanical property mapping mode, tensile testing, and scanning electron microscopy. Miscible blends exhibited Young's modulus and elongation at break values that can significantly extend the usefulness of PLA in commercial applications. The blending of PTM with PLA resulted in films with a 27-fold increase in toughness compared with neat PLA film. © 2014 Wiley Periodicals, Inc. J. Appl. Polym. Sci. **2014**, *131*, 40888.

INTRODUCTION

Thermoformability, energy and weight savings, and durability of polymers make them ideal substitutes for metal, paper, and glass. Since 1976, polymers have been, by weight, the most heavily utilized material globally,[1] but petroleum-based polymers lack the sustainability of renewable polymers. With increased environmental concern and petroleum feedstock costs rising, "green" polymers—those developed from biomass-based resources and those that are degradable—are being sought out as alternatives to petroleum-based polymers. Renewable (bio)-plastics are produced from biomass-derived monomers, and often can be biologically and/or hydrolytically degraded. Products based on recycled and renewable resources are entering the market as toys, packaging materials, clothing, and other goods.[1–6]

There are several types of hydrolytically degradable polymers, including poly(anhydrides), poly(orthoesters), poly(depsipeptides), poly(ether esters), and poly(esters), that are currently being researched as replacements for nonhydrolytically degradable petroleum-based polymers.[7] Poly(esters) have shown to be the most promising candidates for commercialization and replacement of petroleum-based polymers, especially with the development of poly(lactic acid) (PLA), poly(glycolic acid) (PGA), and poly(ε-caprolactone) (PCL). In the 1960s and

1970s, PGA was the first biocompatible and hydrolytically degradable synthetic polymer and was initially commercialized as a dissolvable suture material.[8] This advance spurred research into other biocompatible polymers and into other applications for these polymers. However, performance issues such as poor thermal stability and brittleness were encountered with PLA and PGA.[9,10] To overcome the thermal and mechanical short comings of PLA, PGA, and PCL, polymeric blends and copolymers of said polymers and also with other polymers were examined to enhance the properties with varying degrees of success.[7,9–14]

Blending PLA with plasticizers is one of the most effective approaches for toughening PLA. A variety of plasticizers has been used to improve the mechanical properties of PLA[15]; however, the studies showed significant modulus loss and plasticizer-related problems, such as leaching and phase separation.[16,17] PLA/PCL and PLA/polyhydroxyalkanoate (PHA) blends are two of the most extensively studied PLA blends. Broz et al.[18] reported that the elongation-at-break of PLA increased with the addition of 60 wt % PCL. In another study, Simões et al.[17] found out that addition of PCL to PLA as a plasticizer led to a loss in initial modulus and yield stress, but also an enhancement in the flexibility and ductility of the blend. Moreover, in all PLA/PCL blends, phase separation occurred due to the immiscibility. In the study of Noda et al.,[19] the elongation-

at-break increased to over 100%, and the tensile energy to break also improved 10 times compared with pure PLA with blending of PLA and 10 wt % Nodax, a commercial PHA developed by Procter and Gamble.

Poly(trimethylene malonate) (PTM), developed as part of this study, belongs to the PHAs family and exhibits the same tendencies to degrade hydrolytically, as observed in other PHAs. PTM is a linear, amorphous copolymer composed of ester and ether backbone bonds with a glass-transition temperature of $-57°C$ and a bimodal MW of 1.4 and 34 kDa, making it useful for specialty applications and as a plasticizer. In this study, "green" polymer films made from blends of PLA and PTM were prepared by solvent casting from chloroform. Thermal and mechanical properties of these PLA/PTM films were investigated.

EXPERIMENTAL

Materials
PLA resin (PLA 4042D) was purchased from NatureWorks LLC. The PLA pellets were translucent with a density of 1.24 g/mL. Malonic acid (99%) and chloroform (98%) were used as received from VWR. Aluminum chloride (98%), 1,3-propane diol (98%), and diethyl ether (>99%) were used as received from Sigma-Aldrich (St. Louis, MO). PTM copolymer was synthesized via melt polycondensation as previously described.[20]

Preparation of Blend Films
The PLA resin was dried in a convection oven at 80°C overnight prior to use. PLA and PTM were dissolved separately in chloroform at the concentration of 5% w/w. The solutions were stirred for 12 h at room temperature. PTM was then added to PLA to form final concentrations of 5%, 10%, and 20% w/w. Each PLA–PTM solution was cast into a glass Petri dish, and a lid was placed on top with one side lifted in order to allow for slow solvent evaporation. The cast films were dried at room temperature for 24 h and then vacuum dried at room temperature for 48 h.

Thermogravimetric Analysis
A TA Instruments Q-600 simultaneous DSC/TGA (SDT) was used to characterize the thermal stability of PLA, PTM, and PLA/PTM blend films with the TA Universal Analysis 2000 software (v4.7A). The 5 mg samples were analyzed from room temperature to 400°C at a rate of 10°C/min under a 50 mL/min nitrogen purge.

Differential Scanning Calorimetry
A TA Instruments Q-2000 modulated differential scanning calorimeter was used for thermal analysis of PLA, PTM, and PLA/PTM blend films with the TA Universal Analysis 2000 software (v4.7A). The blend film samples weighing 5 mg were first heated from 40°C to 200°C at a rate of 10°C/min, and then held for 5 min to eliminate the thermal history. Subsequently, they were cooled to $-50°C$, and heated again from $-90°C$ to 200°C at a rate of 10°C/min under 50 mL/min of nitrogen purge. The glass-transition temperature (T_g), melting temperature (T_m), and melting enthalpy (ΔH_m) of the PLA and PLA/PTM blend films were determined from the exotherms, and the
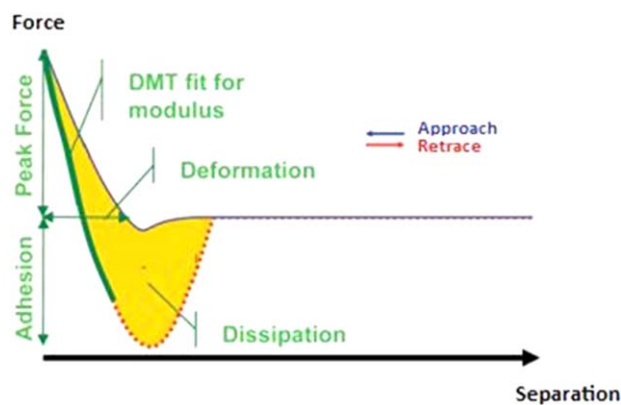

Figure 1. Force–separation curve showing the DMT (Derjaguin–Muller–Toporov) fit to obtain the mechanical properties of the sample. Figure adapted from Ref. 21, with permission from Veeco Instruments Inc. [Color figure can be viewed in the online issue, which is available at wileyonlinelibrary.com.]

degree of crystallinity (X_m) was calculated with the following equation:[17]

$$X_m \ (\%) = \frac{\Delta H_m - \Delta H_{cc}}{\Delta H_0 \ * \ W_f} \times 100 \qquad (1)$$

where ΔH_m is the melting enthalpy of PLA in the blends, ΔH_{cc} is the cold crystallization enthalpy of PLA, ΔH_0 is the melting enthalpy of the 100% crystalline PLA, and W_f is the weight fraction of PLA in the blends. For PLA, the 100% crystalline melting enthalpy was taken to be 93 J/g.[17] The average values of three samples at a minimum are presented.

Atomic Force Microscopy
In this study, an atomic force microscopy (AFM) mode known as PeakForce QNM® (quantitative nanomechanical property mapping) was used on a Dimension Icon atomic force microscope to map the mechanical properties of the bioplastic samples. By using PeakForce Tapping™ damage to the tip and sample can be minimized by directly controlling the forces applied to the tip and using forces lower than those generally used in tapping mode. This method also allows for better control of the maximum force (peak force) on the tip as it ensures that the tip–sample contact area is as small as possible.[21]

During tapping, the AFM generates force curves for each pixel on the sample surface and converts them to the force–separation plots that give some of the major mechanical properties such as elastic modulus, adhesion, dissipation, and deformation. Figure 1 shows the force–separation curve describing the mechanical quantities during a single PeakForce tapping. The Derjaguin–Muller–Toporov (DMT) model can be used to fit the retract curve in order to estimate the reduced modulus, E^*.[21] The DMT model uses eq. (2) with the relationship between modulus and forces given as:

$$E^* = \frac{3}{4}(F - F_{adh}) / \sqrt{R(d - d_0)^3} \qquad (2)$$

where E^* is the reduced elastic modulus of the sample, R is the tip radius, $(F - F_{adh})$ is the difference between the relative forces of the tip and adhesion during the tapping, and $(d - d_0)$ is the

Table I. Thermal Analysis Data of PLA, PTM, and PLA/PTM Blend Films

PLA/PTM weight ratio (wt %)	$T_{5\%}$ (°C)	T_{max} (°C)	T_g (°C)	T_{cc1} (°C)	T_{cc2} (°C)	T_{m1} (°C)	T_{m2} (°C)	ΔH_m (J/g)	ΔH_{cc} (J/g)	X_m (%)	X_{mf} (%)
100/0	332	360	40 ± 2	113 ± 1	–	140 ± 2	–	5.0 ± 0.4	3.8 ± 0.3	1.3 ± 0.8	21.0 ± 0.7
95/5	305	346	31 ± 1	108 ± 3	–	135 ± 1	144 ± 1	17.0 ± 2.8	13.2 ± 2.8	4.2 ± 0.2	19.8 ± 1.4
90/10	295	345	27 ± 2	99 ± 5	–	133 ± 2	144 ± 1	24.5 ± 4.3	22.6 ± 4.4	2.3 ± 0.5	19.6 ± 0.4
80/20	276	338	17 ± 3	68 ± 1	82 ± 1	125 ± 1	142 ± 0	22.7 ± 0.4	17.9 ± 0.7	6.6 ± 1.1	19.3 ± 0.5
0/100	210	340	−57 ± 4	–	–	–	–	–	–	–	–

T_g: glass-transition temperature, T_{m1}: first melting temperature, T_{m2}: second melting temperature, T_{cc1}: first cold crystallization peak temperature, T_{cc2}: second cold crystallization peak temperature, ΔH_{cc}: enthalpy of cold crystallization, ΔH_m: melting enthalpy, X_m: degree of crystallinity, X_{mf}: degree of crystallinity from first heating, $T_{5\%}$: temperature at 5% weight loss, T_{max}: temperature at 50% weight loss.

sample deformation. Young's modulus of the sample (E_s) can be calculated directly from the reduced modulus by using the known Poisson's ratio of the sample.

$$E^* = \left[\frac{1-v_s^2}{E_s} + \frac{1-v_{tip}^2}{E_{tip}} \right]^{-1} \tag{3}$$

where E_s is the Young's modulus of the sample, E_{tip} is the modulus of the tip, and v_s and v_{tip} are the Poisson's ratios of the sample and the tip, respectively. Here, the elastic modulus of the tip (E_{tip}) can be assumed infinite.[21]

AFM PeakForce QNM measurement mode was performed using a Dimension ICON AFM with a RTESPA probe (40 N/m spring constant, 10 nm tip radius) to map the topography and mechanical properties of the bioplastic blend samples. PLA, PTM, and PLA/PTM blend samples were attached to the metal AFM pan using adhesive tape. The scanning rate was <1 Hz, and the scan size was 5 × 5 μm (512 × 512 pixels). The peak-force set-point and the Poisson's ratio were set to 3.0 μN and 0.3, respectively. AFM images were analyzed with NanoScope Analysis software (v1.40). Average values of a minimum of three measurements are presented.

Mechanical Analysis

Tensile tests were carried out to measure the mechanical properties of PLA and PLA/PTM blend films. The tests were performed on an Instron 5869 electromechanical universal testing machine with a 50-kN load cell in accordance with ASTM D882-10. The rectangular specimen samples (50 × 5 × 0.40 mm) were stored in ambient conditions. A crosshead speed of 6 mm/min and an initial distance between grips of 35 mm were used. Three specimens of each sample were tested, and the average values are presented.

Scanning Electron Microscopy

The tensile fracture surfaces of PLA and PLA/PTM blend films were studied by a JEOL JSM-6500F field emission scanning electron microscope at 5 kV. The films were mounted onto the metal pan using adhesive tape, and then an EMS 150T ES coater was used to sputter the film surfaces with 5 nm of platinum to reduce electrostatic charging.

Statistical Analysis

The results are described as mean and standard deviation (mean ± SD). The statistical analysis was performed by the one-way analysis of variance (ANOVA), Tukey's method of multiple comparisons at a significance level of less than 0.05 ($P < 0.05$) using MINITAB®.

RESULTS AND DISCUSSION

Thermal Properties

The thermal behavior of the solvent-cast films of PLA, PTM, and PLA/PTM blends was analyzed by differential scanning calorimetry (DSC), and the data are summarized in Table I. The second heating thermograms are shown in Figure 2. Neat amorphous PTM has a glass-transition temperature of −57°C ± 4°C. Neat PLA cast film has a single melting temperature of 140°C ± 2°C, and a glass-transition temperature of 40°C ± 2°C. A very weak cold crystallization peak of the neat PLA was observed, and its cold crystallization temperature was around 113°C ± 1°C. A single glass-transition temperature of the blend films can indicate the miscibility of the two polymers. The glass-transition temperature of the blends was decreased with addition of PTM into PLA matrix that can be explained with PTM's plasticizer behavior. In Figure 2, for PLA/PTM blends, a double peak melting point appeared around 135°C ± 1°C and 144°C ± 1°C. The melting temperatures of PLA film shifted and increased slightly by blending with PTM.

Double or multiple melting peaks have been observed during DSC measurements in semicrystalline polymers including
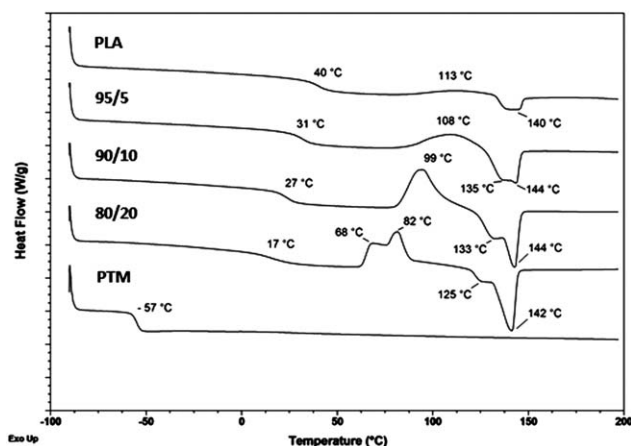

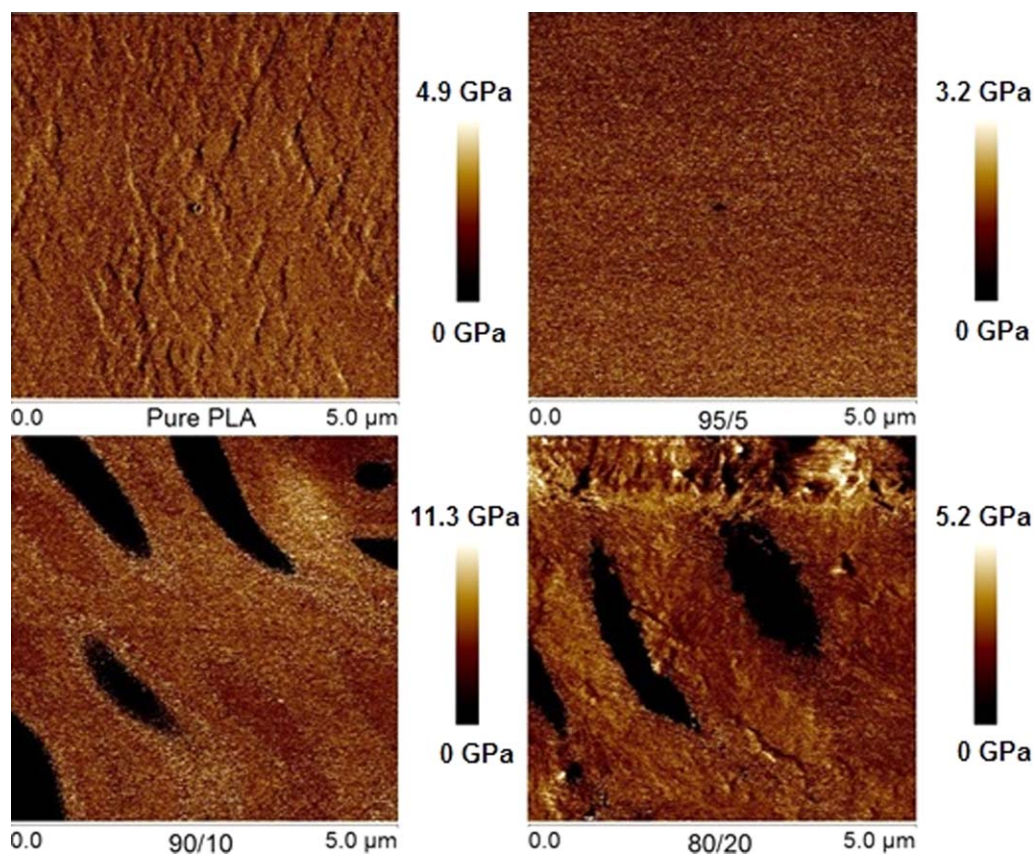**Figure 2.** DSC thermograms of PLA, PTM, and PLA/PTM blend films from the second heating cycle.

Figure 3. AFM DMT (Derjaguin–Muller–Toporov) modulus maps ($5 \times 5\ \mu m^2$) of neat PLA and PLA/PTM blends. [Color figure can be viewed in the online issue, which is available at wileyonlinelibrary.com.]

poly(butylene terephthalate),[22] poly(phenylene sulfide),[23] nylon-6,[24] and PLA.[25–27] Double melting peaks have been explained by the presence of multiple crystalline morphologies, the presence of multiple crystal modifications, the melting–recrystallization–remelting processes, the fusion of the lamellae with smaller thickness, and/or heterogeneous nucleation.[25,28] Several investigators have observed double melting peaks during DSC scans of PLA samples and its blends.[25–27,29] In a DSC analysis of PLA/talc composites, Jain et al.[25] reported that the double melting peaks are attributed to heterogeneous nucleation effect of talc particles on PLA surfaces, leading to the formation of two types of crystal structures. In another study, Yasuniwa et al.[26] performed a thermal analysis of the melting and crystallization processes to investigate the double-melting behavior of poly(L-lactic acid) (PLLA), and attributed the double peaks to a melting–recrystallization–remelting mechanism. During the melting–recrystallization–remelting mechanism, the imperfect and small crystals could melt and recrystallize to form more stable crystals. It suggests that the lower-temperature and higher-temperature melting peaks correspond to the melting of the primary crystallites and the melting of the recrystallized crystallites formed during the DSC heating scan, respectively.[28]

The cold crystallization peak became narrower, decreasing with increasing PTM content, and was bimodal at 20% of PTM. Such a change in crystallization was reported by Pillin et al.[30] and Wu et al.[31] They observed a strong decrease in crystallization temper-

ature for plasticized PLA and polyvinyl alcohol. The degree of crystallinity (X_m) for PLA and the PLA/PTM blends was determined using eq. (1) and is listed in Table I. The melting enthalpy and cold crystallization enthalpy from the second heating cycle were used to find the degree of crystallinity of each sample. It was found to be 1.3% ± 0.8% for neat PLA and 4.2% ± 0.2% for a PLA/PTM blend with 5 wt % of PTM. The degree of crystallinity of cast PLA film increased with increasing PTM content. This may indicate that PTM serves as a nucleating agent. The findings of DSC analysis that PTM has simultaneously served as a plasticizer and a nucleating agent of PLA may be related to the bimodal MW distribution observed in the PTM sample. The degree of crystallinity was also calculated from the first heating

Table II. Average Elastic Modulus (E) of PLA, PTM, and PLA/PTM Blend Films ($5 \times 5\ \mu m^2$)

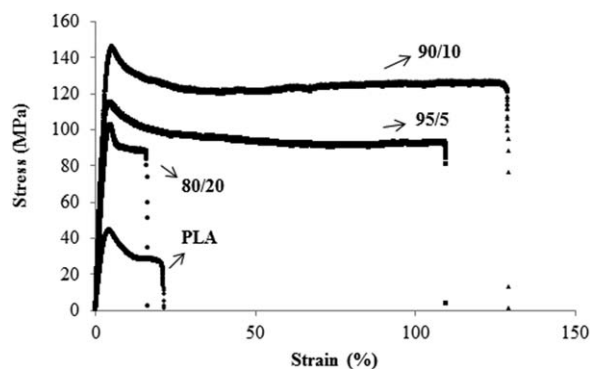| PLA/PTM weight ratio (wt %)	DMT modulus at 25°C (GPa)	DMT modulus at 90°C (GPa)
100/0	2.66 ± 0.24	–
95/5	2.98 ± 0.49	1.27 ± 0.02
90/10	7.30 ± 0.37	1.31 ± 0.04
80/20	4.09 ± 0.67	1.50 ± 0.38
0/100	0.007	–

DMT: Derjaguin–Muller–Toporov.

Figure 4. Stress–strain curves of PLA and PLA/PTM blend films.

cycle. It showed higher values than those from the second heating cycle and decreased slightly with PTM addition.

Thermal stability of solution-cast PLA and PLA/PTM blend films was investigated by thermogravimetric analysis. In Table I, the temperature where 5 wt % loss is attained ($T_{5\%}$) and the maximum working temperature where 50 wt % loss occurs (T_{max}) are both listed for each sample. Thermal stability of PLA/PTM blends cast from chloroform was found to be less than that of neat PLA. Thermal degradation temperatures of $T_{5\%}$ and T_{max} for neat PLA films were 332°C and 360°C, respectively, and were similar to those of PLA resin. It seemed that thermal stability of neat PLA was not affected by the solvent casting process.

Nanomechanical Properties

In this study, nanomechanical properties of neat PLA and PLA/PTM blends were investigated by AFM PeakForce QNM. By AFM, both qualitative and quantitative topographical and nanomechanical information can be obtained. The elastic modulus of the blends was determined using the DMT model. PeakForce QNM-DMT modulus maps ($5 \times 5 \ \mu m^2$) of the neat PLA and PLA/PTM cast blend films are shown in Figure 3. The tensile modulus of extruded neat PLA films provided by NatureWorks was 3.3 GPa.[32] In this work, average DMT modulus of the neat PLA films was measured to be 2.66 ± 0.24 GPa. High modulus areas with lighter colors are visible in the PLA crystalline structure whereas darker colors are representative of low modulus areas of the amorphous phase. The 95/5 PLA/PTM blend (with 5 wt % PTM) is similar to the neat PLA and has a smooth surface with a uniform modulus. As the amount of PTM was increased from 5 to 10 wt %, dark, low-modulus areas can be seen in the PLA matrix. The regions are shaped from ovoid to a

linear "tiger paw" stripes and have a very low modulus of 47 MPa indicating only PTM (or empty voids) is present. The lighter areas with a modulus of approximately 8.05 GPa are much harder than the neat PLA surface and may be ascribed to the higher number of ester bonds and the higher degree of crystallinity in the blends. The modulus maps of the 80/20 PLA/PTM blend films (with PTM content of 20 wt %) is similar to that obtained for the blend with 10 wt % PTM. The PTM domains or empty voids are a significant portion of the surface and lower the average DMT modulus to 4.09 ± 0.67 GPa (Table II). AFM-PeakForce QNM analysis was also performed on PLA/PTM blend films at 90°C to investigate the impact of elevated temperature on modulus. The results show that the moduli of all blends decreased significantly at 90°C (Table II).

Tensile Properties

The macroscale mechanical properties of PLA and PLA/PTM blend films were studied to investigate the effect of PTM on the tensile strength, elongation-at-break, Young's modulus, and toughness. The tensile stress–strain curves of PLA and PLA/PTM blends are shown in Figure 4. The stress–strain curves of the blends showed a ductile material behavior, and the blend films had a significant increase in tensile strength and elongation-at-break compared with neat PLA films.

The detailed mechanical properties are presented in Table III with the statistical analysis. Incorporation of PTM increased the tensile strength and showed the same trend as was observed for the Young's modulus values. Maximum average values of 105.61 ± 19.76 MPa for tensile strength and 4.61 ± 0.72 GPa for Young's modulus were observed, respectively, at 10 wt % PTM. Because of the phase separation/debonding observed, the Young's modulus decreased by 36% as PTM content was increased from 10 to 20 wt %. Therefore, the Young's modulus results are correlated with the miscibility of PLA and PTM. This is highly notable, as PTM is a soft and waxy amorphous copolymer with an elastic modulus of around 7 MPa. It was anticipated that PTM would behave as a plasticizer for PLA, and reduce PLA's Young's modulus but increase its elongation-at-break. However, incorporation of PTM into the PLA matrix improved PLA's mechanical properties until a miscibility/solubility limit was reached.

Another important mechanical property, elongation-at-break, can be observed in the stress–strain curves (Figure 4 and Table III). Elongation-at-break increased with increasing PTM wt % in the blends, and 10 wt % was found to be the optimum level that gave the largest elongation-at-break of $116.55\% \pm 16.53\%$, which is about seven-fold of that for the neat PLA films.

Table III. Tensile Testing Data of PLA and PLA/PTM Blend Films

PLA/PTM weight ratio (wt %)	Tensile strength (MPa)	Strain at break (%)	Young's modulus (GPa)	Toughness (MPa)
100/0	21.20 ± 8.74 (B)	15.59 ± 4.69 (B)	1.69 ± 0.60 (B)	5.39 ± 1.75 (C)
95/5	83.24 ± 8.48 (A)	107.69 ± 6.42 (A)	4.01 ± 0.12 (A)	92.48 ± 15.86 (B)
90/10	105.61 ± 19.76 (A)	116.55 ± 16.53 (A)	4.61 ± 0.72 (A)	143.53 ± 22.97 (A)
80/20	71.79 ± 23.27 (A)	13.37 ± 2.75 (B)	2.96 ± 0.90 (A, B)	11.71 ± 2.35 (C)

Letters in the bracket correspond to results generated by one-way analysis of variance using Tukey's method of multiple comparisons. Means that do not share a letter are statistically different from one another.
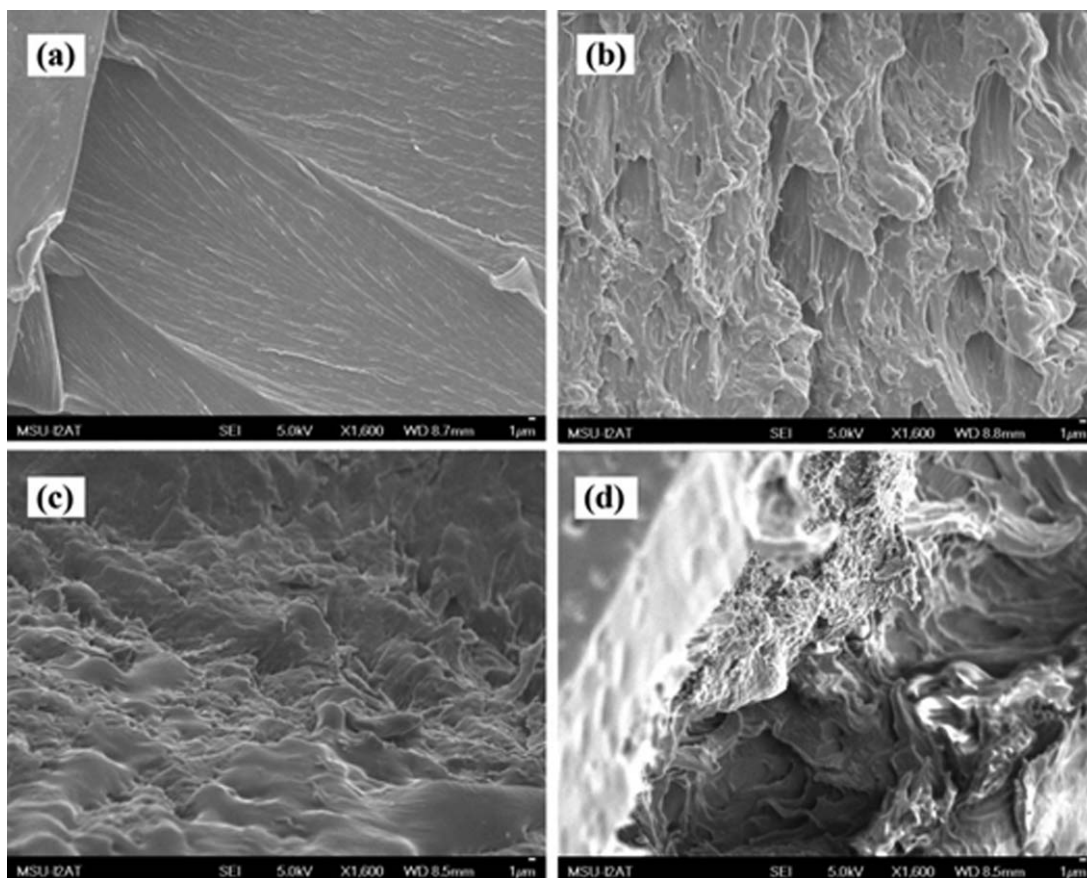
Figure 5. SEM micrographs (×1600) of the fracture surfaces of tensile specimens of (a) PLA, (b) 95/5 PLA/PTM blend, (c) 90/10 PLA/PTM blend, and (d) 80/20 PLA/PTM blend films.

Incorporation of PTM into PLA at levels below 20 wt % demonstrated an increase in key mechanical properties; however, at a 20 wt % loading of PTM, the PTM addition starts to show a negative impact due to phase segregation/debonding. Toughness of the blends was determined by integration of the area under the stress–strain curves, and was performed using OriginPro 8 (v8.0). Addition of 5 and 10 wt % PTM into PLA resulted in a significant toughness increase due to an increase in both the measured tensile strength and elongation-at-break. The toughness increased from 5.39 ± 1.75 MPa for neat PLA to 143.53 ± 22.97 MPa for the blend with 10 wt % PTM.

As a result, miscible blends (less than 20 wt % PTM) of PTM in PLA exhibited Young's modulus and elongation at break values that significantly extend the range of applications for PLA. For example, PLA with 10 wt % PTM demonstrated tensile strength comparable with polyamide-imide, a Young's modulus that exceeds polyamide-imide, and elongation at break greater than polypropylene, polycarbonate, and nylon 6.[33]

Scanning Electron Microscopy
Scanning electron microscopy (SEM) was used to analyze the fracture surface morphology of the tensile specimens. Figure 5(a–d) shows the SEM micrographs of the tensile fractured surfaces. A number of small cleavage planes are observed in Figure 5(a), corresponding to a brittle failure. In Figure 5(b,c), there were no separate domains of PLA and PTM with spherical

shape morphology, indicative of miscible polymer blends. In the micrographs of the blends with 5 and 10 wt % PTM, cavities were observed with different sizes depending on the PTM ratio. The presence of these cavities may be caused by debonding. These cavities can cause high tensile strength by consuming more energy during the fracture as seen in a tensile study.[34] The micrograph of the blend with 20 wt % PTM [Figure 5(d)] revealed significant cavitation caused by debonding. Therefore, lower ratios of PTM in these blends resulted in effective dispersion of PTM in the PLA matrix and avoid debonding/phase separation. These results are consistent with the AFM and tensile data.

CONCLUSIONS

PLA and PLA/PTM "green" blend films were prepared by the solvent-casting method from chloroform. Thermal properties of the blend films were investigated by DSC and thermogravimetric analysis. In addition to standard AFM scanning, PeakForce QNM was used to map the morphology and nanomechanical properties. The addition of PTM increased the degree of crystallinity for the blends. The shifting of the melting temperatures of PLA film by blending with PTM, along with a single glass-transition temperature observed for the blends, indicate that the two degradable polymers were miscible. Addition of PTM gave the blends higher modulus and elongation-at-break compared

with those of neat PLA films, and the toughness was improved significantly. Phase separation/debonding was identified in the blends with PTM contents of 10 and 20 wt %; however, even though the Young's modulus for the 20 wt % blend had decreased compared with the lower PTM/PLA ratio blends, it was still a higher value than that of neat PLA. These PTM/PLA bioplastic blends have shown much improved mechanical properties, which can lead to easier and more economical processing, reduced packaging volume, and expanded commercial application.

ACKNOWLEDGMENTS

REFERENCES

1. Mapleston, P. *Plast. Eng.* **2008**, *64*, 10.

2. Robinson, G. *Waste Manag. World* **2007**, 77.

3. Pandey, J. K.; Ahn, S.; Lee, C. S.; Mohanty, A. K.; Misra, M. *Macromol. Mater. Eng.* **2010**, *295*, 975.

4. Stewart, R. *Plast. Eng.* **2008**, *64*, 17.

5. Inman, H. *Plast. Eng.* **2010**, *66*, 42.

6. Keshavarz, T.; Roy, I. *Curr. Opin. Microbiol.* **2010**, *13*, 321.

7. Neffe, A. T.; Tronci, G.; Alteheld, A.; Lendlein, A. *Macromol. Chem. Phys.* **2010**, *211*, 182.

8. Chu, C. *J Appl. Polym. Sci.* **1981**, *26*, 1727.

9. Quynh, T. M.; Mitomo, H.; Yoneyama, M.; Hien, N. Q. *Polym. Eng. Sci.* **2009**, *49*, 970.

10. Shirahase, T.; Komatsu, Y.; Tominaga, Y.; Asai, S.; Sumita, M. *Polymer* **2006**, *47*, 4839.

11. Catıker, E.; Gümüşderelioğlu, M.; Güner, A. *Polym. Int.* **2000**, *49*, 728.

12. Hill, S. P.; Montes de Oca, H.; Klein, P. G.; Ward, I. M.; Rose, J.; Farrar, D. *Biomaterials* **2006**, *27*, 3168.

13. Höglund, A.; Odelius, K.; Hakkarainen, M.; Albertsson, A.-C. *Biomacromolecules* **2007**, *8*, 2025.

14. Oyama, H. T.; Tanaka, Y.; Kadosaka, A. *Polym. Degrad. Stab.* **2009**, *94*, 1419.

15. Anderson, K. S.; Schreck, K. M.; Hillmyer, M. A. *Polym. Rev.* **2008**, *48*, 85.

16. Zhang, J.-F.; Sun, X. *Polym. Int.* **2004**, *53*, 716.

17. Simões, C. L.; Viana, J. C.; Cunha, A. M. *J. Appl. Polym. Sci.* **2009**, *112*, 345.

18. Broz, M. E.; VanderHart, D. L.; Washburn, N. R. *Biomaterials* **2003**, *24*, 4181.

19. Noda, I.; Satkowski, M. M.; Dowrey, A. E.; Marcott, C. *Macromol. Biosci.* **2004**, *4*, 269.

20. Rowe, M. D.; Walters, K. B. In 67th Annual Technical Conference of Society of Plastic Engineering; Society of Plastics Engineers (SPE): Chicago, IL **2009**; p 508.

21. Pittenger, B.; Erina, N.; Su, C. Quantitative mechanical property mapping at the nanoscale with PeakForce QNM. Application Note Veeco Instruments Inc. http://www.bruker-axs.com/uploads/tx_linkselectorforpdfpool/Quantitative_Mechanical_Property_Mapping_at_the_Nanoscale_with_PeakForce-QNM_AFM_AN128.pdf. Accessed November 12, 2011.

22. Yasuniwa, M.; Tsubakihara, S.; Murakami, T. *J. Polym. Sci. Part B Polym. Phys.* **2000**, *38*, 262.

23. Breach, C. D.; Hu, X. *J. Mater. Sci. Lett.* **1996**, *15*, 1416.

24. Todoki, M.; Kawaguchi, T. *J. Polym. Sci. Polym. Phys. Ed.* **1977**, *15*, 1067.

25. Jain, S.; Misra, M.; Mohanty, A.; Ghosh, A. *J. Polym. Environ.* **2012**, *20*, 1027.

26. Yasuniwa, M.; Tsubakihara, S.; Sugimoto, Y.; Nakafuku, C. *J. Polym. Sci. Part B Polym. Phys.* **2004**, *42*, 25.

27. Li, Y.; Wu, H.; Wang, Y.; Liu, L.; Han, L.; Wu, J.; Xiang, F. *J. Polym. Sci. Part B Polym. Phys.* **2010**, *48*, 520.

28. Supaphol, P. *J. Appl. Polym. Sci.* **2001**, *82*, 1083.

29. Lee, J. K.; Lee, K. H.; Jin, B. S. *Eur. Polym. J.* **2001**, *37*, 907.

30. Pillin, I.; Montrelay, N.; Grohens, Y. *Polymer* **2006**, *47*, 4676.

31. Wu, W.; Tian, H.; Xiang, A. *J. Polym. Environ.* **2012**, *20*, 63.

32. Technical Data Sheet of NatureWorks® PLA Polymer 4042D. Available at: http://www.natureworksllc.com Accessed March 5, 2012.

33. Matweb: Material Property Data. Available at: http://www.matweb.com/reference/tensilestrength.aspx Accessed June 19, 2013.

34. Prolongo, S. G.; Campo, M.; Gude, M. R.; Chaos-Morán, R.; Ureña, A. *Compos. Sci. Technol.* **2009**, *69*, 349.